

SHAKEDOWN ANALYSIS OF “SOIL-PILE FOUNDATION-FRAME” SYSTEM UNDER SEISMIC ACTION

Piotr ALAWDIN¹, George BULANOV²

¹ University of Zielona Gora, Zielona Góra, Poland

² RUP "Instytut BelNIIS", Minsk, Belarus

Abstract

In this article, the seismic shakedown FEM analysis of reinforced concrete and composite spatial frame structures on the deformable foundation, taking into account the elastic-plastic and brittle behavior of structures elements, is presented. A foundation consists of group of the piles in the soil. The behavior of soil is described here using+ the elastic half-space theory. The pile deformation model is assumed to be elastic-perfectly plastic, where the bearing capacity is determined by the results of testing the soils or the piles themselves. An example of seismic shakedown limit analysis is presented.

Keywords: seismic shakedown limit analysis, soil-structure interaction, frames, piles foundation, elastic-plastic and brittle elements

1. INTRODUCTION

There are many different technics to consider soil-structure interaction [1]. As usually, design of structures for earthquake resistance considering soil-structure interaction is very complicated problem requiring a sufficiently long computation time and having a large number of uncertainties and assumptions [12-16]. As an alternative, the shakedown [17-19] seismic analysis of structures, taking into account the elastic-plastic and brittle behavior of their elements, was presented in the work [2]. In this article, such seismic shakedown analysis of structures is proposed to be performed taking into account the soil-structure interaction.

¹ Corresponding author: University of Zielona Gora, Faculty of Civil Engineering, Architecture and Environmental Engineering, Szafrana st 1, 65-516 Zielona Góra, Poland, e-mail: p.aliawdin@ib.uz.zgora.pl, tel.+48683282322

The stiffness matrix representing the soil part of the soil-foundation-structure interaction system has been calculated based on the elastic half-space theory. The pile deformation model is assumed to be elastic-perfectly plastic, where the bearing capacity is determined by the results of testing the soils or the piles themselves.

2. MATHEMATICAL MODEL

2.1. Mathematical formulation of optimization problem

The problem of load-bearing capacity of structures made of perfectly elastic-plastic and elastic-brittle elements taking into account soil-structure interaction, under variable actions is formulated as follows. Find a parameter (safety factor) μ for load F , as well as the vector of residual forces such, that

$$\mu \rightarrow \max, \quad (2.1)$$

$$S^e(t) = f(\mu F(t)), \quad (2.2)$$

$$K_s q + K^d E_p d = 0, \quad (2.3)$$

$$\varphi_{pl}(S^e(t) + S_p^r, S_{0,pl}) \leq 0, \quad (2.4)$$

$$\varphi_{br}(S^e(t), S_{0,pl})_i \leq 0, \quad i \in I_{br}, \quad (2.5)$$

$$\varphi_{pl}(N_{pile}^e(t) + N_{pile}^r(q), N_{pile,pl}) \leq 0 \quad (2.6)$$

$$F(t) \in \Omega(F_j(t), t), \quad (2.7)$$

where S^e, S^r are the vectors of elastic and residual internal forces in the cross sections of elements; $S_{0,pl}, S_{0,br}$ - vectors of limit internal forces in the cross sections of elastic-plastic and elastic-brittle elements accordingly; N_{pile}^e, N_{pile}^r - vectors of elastic and residual normal forces acting on the piles; $N_{pile,pl}$ - vectors of limit internal forces in the piles equal to bearing capacity of the piles; d - a vector of distortions in the elements; $F(t)$ - a vector of load; I_{br} - set of i -th brittle elements; $\Omega(\bullet)$ - set of loads $F(t)$, t - time; K_s - soil stiffness matrix linked with structural part; q - vector of unknowns of FEM (usually as element

displacements), \mathbf{K}^d - matrix of influence of distortions \mathbf{d} on the reaction of finite elements; \mathbf{E}_p – matrix of partial redistribution of residual forces \mathbf{S}^r [2],

$$E_p = \text{Diag} \begin{bmatrix} 1 & \text{if plastic element} \\ 0 & \text{if brittle element and } \varphi_{br}(\cdot)_i = 0, \quad i \in I_{br} \end{bmatrix}. \quad (2.8)$$

2.2. Mathematical formulation of optimization problem

For elastic-plastic element we observed some ductility. And for an elastic-brittle element we considered sudden collapse.

The inequality constraint (5) in the case of brittle damage, for instance, due to normal or shear forces may be written consequently as

$$N_{ed} \geq N_{rd}(M_{ed}) \text{ or } V_{ed} \geq V_{rd} \quad (2.9)$$

V_{ed} = shear force in the element; V_{rd} = shear resistance of the element; N_{ed} = normal force in the element; $N_{rd}(M_{ed})$ = normal force resistance of the element according to N-M interaction diagram.

No additional conditions other than (5,9) are required for hinges with force-controlled actions (N,V) [3].

We considered curvatures/rotation angles in sections of elements as distortions \mathbf{d} . Furthermore, we can also limit deformations in plastic hinges with deformation-controlled action (M). For this we add the additional inequality constraint:

$$N_{ed} \geq N_{rd}(M_{ed}) \text{ or } V_{ed} \geq V_{rd} \quad (2.10)$$

where $\boldsymbol{\theta}^e$ = a vector of elastic rotation angles in sections of elements; $\boldsymbol{\theta}^p$ = a vector of plastic rotation angles in sections of elements.

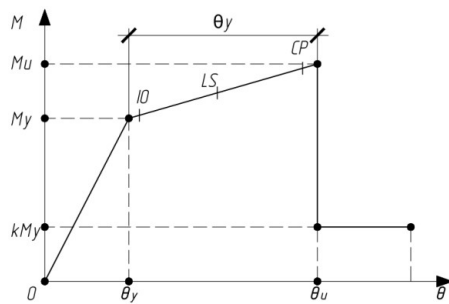


Fig. 1. Moment-rotational angle diagram for plastic element

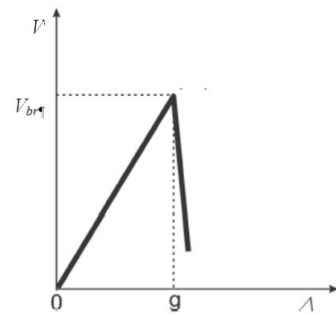


Fig. 2. Shear force-displacement diagram for brittle element

3.1. Soil behaviour

The stiffness matrix representing the soil part of the soil-structure interaction system has been calculated based on the half-space theory [4]. Then the soil stiffness matrix is linked with the structure part and the response of the entire system under the prescribed loads or distortions is calculated.

For point loads P acting on half-space (Figure 3(a)) or within the half-space (Figure 3(b)), accordingly for pile foot forces or pile skin friction forces, vertical stresses σ_z are computed according [5]. With the known stress state and known material properties of the half-space it is possible to compute the vertical strains $\varepsilon_z(z)$. Corresponding vertical displacement (settling) of the soil point at the depth z is obtained by integrating strains from z_{max} (e.g. rigid boundary) up to the level z .

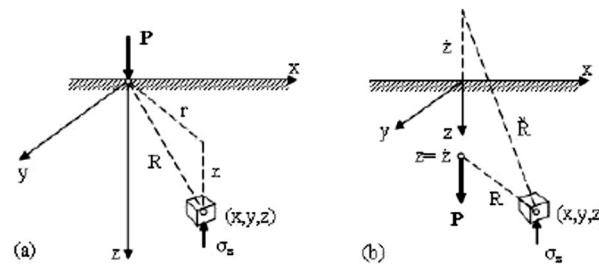


Fig. 3. Stresses in vertical direction σ_z under a center point of the circular pressure load σ_o acting on the half-space surface

The pile deformation model is assumed to be elastic perfectly-plastic, where the bearing capacity $R_{c,d}(N_{pile,pl})$ is determined by the results of testing the soils or the piles themselves (see Figure 4).

Some attention should be paid to determining the dynamic deformation modulus of the soils for a more realistic simulation of the interaction of the soil-structure under seismic action.

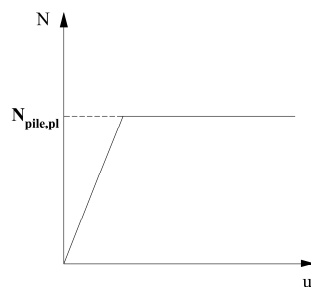


Fig. 4. Normal forces-displacement diagram for the pile

3. EXAMPLE OF SHAKEDOWN ANALYSES OF COMPOSITE FRAME

3.1. FEM model

An example of shakedown analysis of spatial composite steel-reinforced concrete braced frame with elastic-plastic and elastic-brittle elements considering soil-structure interaction is shown in Figure 5.

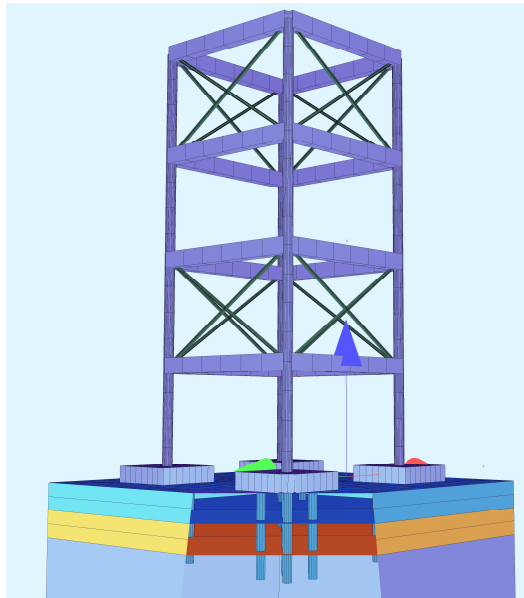


Fig. 5. Model of the frame with pile foundation

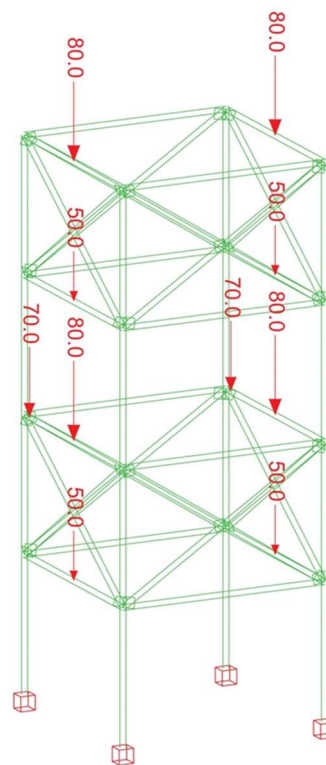


Fig. 6. Live load on the structure

3.2. Seismic action and load combinations

The first step is to define the envelope of internal forces from arising seismic action in elastic stage of work. Seismic action is presented in the form of an elastic response spectrum. For this we use type 1 elastic response spectrum for ground type D, given in Eurocode 8. Peak ground acceleration is equal 0.55 m/s^2 . We do not use the behavior factor for the calculation, since the

nonlinear properties of materials are taken into account directly [6]. The natural frequencies and vibration modes for calculating the response of the structure are given in Table 1.

Response of structure to earthquake excitation we can compute as follows:

1. Define the structural properties
 - Determine the mass matrix m and the stiffness matrix k
 - Estimate the modal damping ratios ζ_n (was accepted at a rate of 5% in this example)
2. Determine the natural frequencies ω_n and natural modes ϕ_n of vibration (table 1)
3. Compute the peak response in the n-th mode:
 - Determine A_n (acceleration ordinate) and D_n (displacement ordinate) from the response or design spectrum corresponding to natural period T_n and damping ratio ζ_n
 - Compute the displacements with $u_{jn} = \Gamma_n \phi_{jn} D_n$
 - Compute equivalent static forces f_n from $f_{jn} = \Gamma_n m_j \phi_{jn} A_n$
 - Compute the story forces, shear and overturning moment, and element forces, bending moments and shear, by static analysis of the structure subjected to lateral forces f_n
4. Determine an estimate for the peak value r of any response quantity by combining the peak modal values r_n according to square root of the sum of the squares (SRSS) or complete quadratic combination (CQC).

For each critical load and action cases, the design values of internal forces were determined by combining action for seismic design situation in according with Eurocode 0 [7]:

$$Ed = G_{kj,\text{sup}}(G_{kj,\text{inf}}) + A_{ed} + \psi_{2,i} Q_{k,i} \quad (3.1)$$

$G_{kj,\text{sup}}(G_{kj,\text{inf}})$ = unfavourable (favourable) characteristic of permanent action (see Figure 3), A_{ed} = design seismic action, $\psi_{2,i}$ = factor by A1.2.2 [7], $Q_{k,i}$ = accompanying variable actions.

3.3. Material and element properties

Design model is shown in Figure 5, the cross-sections of the frame elements are exposed in Table 1; strength class for concrete is C35/45.

Design value of the element (section) resistance was determined according to Global Resistance Factor method described in Fib Model Code 2010 [8]:

$$R_d = R(f_{cR}, f_{yR}, f_{uR})/\gamma_R, \quad (3.2)$$

where γ_R =global safety coefficient is equal 1,3; $f_{cR} = 0,85 \cdot \alpha \cdot f_{ck}$; $\alpha=1$; $f_{yR} = 1,1$; $f_{yk}, f_{tR} = 1,08 \cdot f_{yR}$.

The concrete stress-strain diagram is assumed to be parabolic according to Eurocode 1992-1-1, but modified for use in non-linear ULS calculations. The steel stress-strain diagram is assumed to be bilinear, modified for nonlinear calculations in ULS. Modified material stress-strain diagrams are shown in the Figures 7, 8.

For high intense earthquake, if speed of increasing compressive stresses or strains is at a constant range of approximately $1 \text{ MPa/s} < |\dot{\sigma}_c| < 10^7 \text{ MPa/s}$ and $30 \cdot 10^{-6} \text{ s}^{-1} < |\dot{\epsilon}_c| < 30 \cdot 10^{-2} \text{ s}^{-1}$, we can use provisions given in subclauses 5.1.11.2.1 of Model Code 2010. With their help, we can take into account stress and strain rate effects. The plastic moment capacity of all composite concrete members was calculated by moment-rotation (curvature) analyses according to [9]. The moment-rotation curve can be idealized with an elastic perfectly plastic response to estimate the plastic moment capacity of a member's cross-section [10]. The plastic moment capacity for members' cross-sections have shown in Table 2.

For columns, it is necessary to take into account the possibility of both brittle fracture due to crushing of concrete and plastic failure due to yielding of the tension reinforcement. For this purpose, we need to build the N-M interaction diagram for elements under compression and bending. The interaction of N-M is taken into account both in moment-rotation (curvature) analyses of the plastic moment capacity and in the solution of the optimization problem as a condition for brittle fracture (2.9).

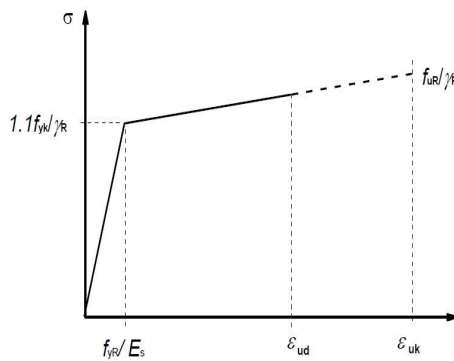


Fig. 7. Stress-strain diagram for steel for analysis in ULS

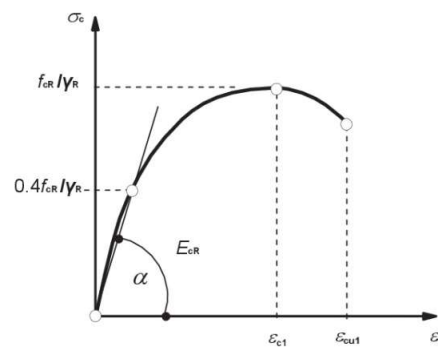


Fig. 8. Stress-strain diagram for concrete for analysis in ULS

Table 1. Sections of frame members

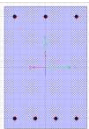
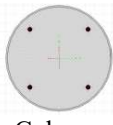
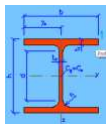
№	Section	b(D), mm	H, mm	Longitudinal reinforcement, class		Steel section, class
				top	bottom	
1.	 Beam	400	600	3Ø16, B500B	4Ø16, B500B	
2.	 Column	400		4Ø16, B500B		RO 377x6, S235
3.	 rod brace					HE100A, S275

Table 2. The plastic moment capacity for members' cross-sections

Number of cross-section in Table 1 (axial force N, kN)	The plastic moment capacity M_p for positive moment, $kN \cdot m$	The plastic moment capacity M_p for negative moment, $kN \cdot m$
1	192	146.5
2 (-574)	284	284
2 (-197)	276	276

Transverse reinforcement of all concrete beams is made from bars Ø8 B500B at 200 mm (Figure 4). Resistance of the concrete beams to vertical shear designed in according with Eurocode 2 [11]. Design shear capacity $V_{Rd,s}$ is equal 226.7 kN. Resistance of the composite columns to vertical shear designed in according with Eurocode 4 [9]. The distribution of the total vertical shear V_{Ed} into the parts $V_{a,Ed}$ and $V_{c,Ed}$, acting on the steel section and the reinforced concrete core of the composite columns respectively assumed to be in the same ratio as the contributions of the steel section and the reinforced concrete core to the bending resistance $M_{pl,Rd}$ (see Table 3). Envelope diagram of shear forces is shown in Figure 5. Some structural drawings and views of the frame illustrated in Figures 9,10.

Table 3. Shear resistance of composite column

Part of section	Shear resistance, V_{Rd} , kN	Bending resistance $M_{pl,Rd}$, $kN\cdot m$	Shear force (max) V_{Ed} , kN
Concrete core	296	102	30.2
Steel tube	630	202	60.4

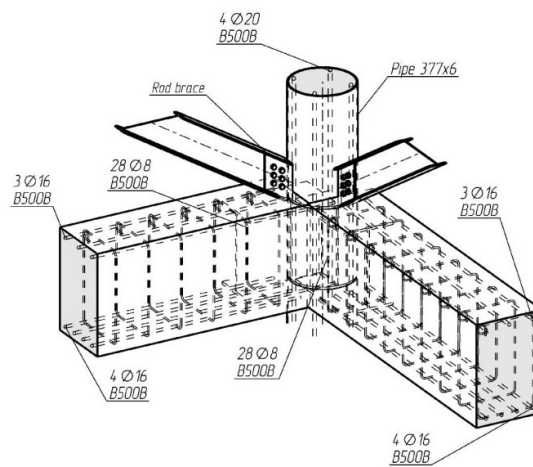


Fig. 9. Structural drawings of the frame joint

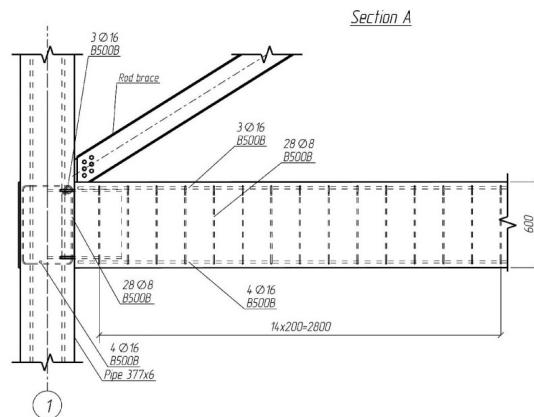


Fig. 10. View of the frame joint

3.4. Material and element properties

Envelope diagram of shear forces is shown in Figure 11. Envelope diagram of elastic bending moments is shown in Figures 13,14.

To solve the optimization problem first we have to find independent residual forces from the residual distortions (curvature) k_r in cross-sections of the elastic-plastic elements.

By solving nonlinear optimization problem as sequence of linear programming tasks, we obtain the solution of optimization problem. Interaction between the moment capacity and the axial force (see Figure 12) was taken into account for the second iteration and the safety factor for load $\mu = 1,19$ was obtained.

The results of shakedown analysis are presented on Figures 15, 16 and they compared with elastic analysis (without safety factor) in Table 4. The results of optimization of normal forces in the piles are presented on Figure 18 and forces in elastic stage are presented on Figure 17 for compare. Shakedown analysis shows us redistribution of moments from the side to the center section of the bottom (at the first floor) beam that makes better use of their load-bearing capacity.

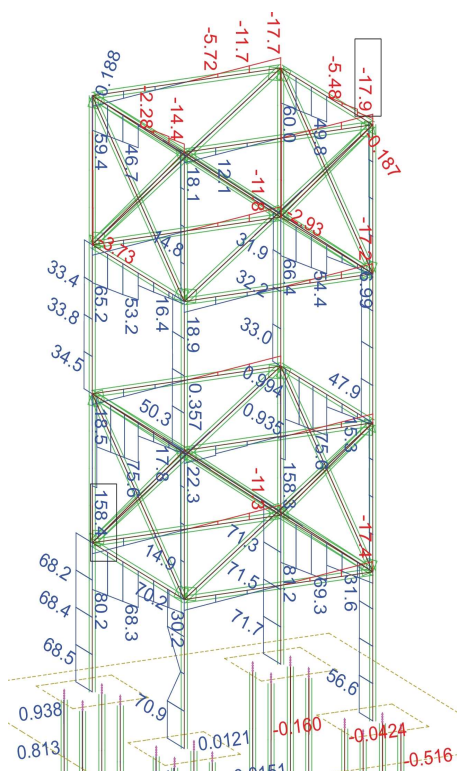


Fig. 11. Envelope diagram of shear forces (max value), kN

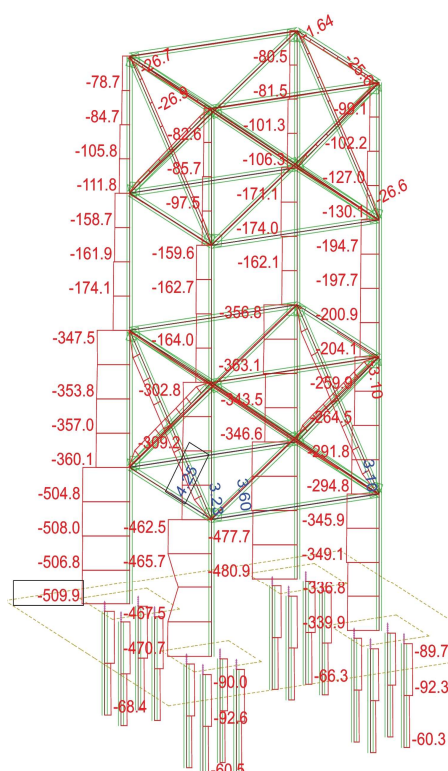


Fig. 12. Envelope diagram (min value) of axial forces, kN

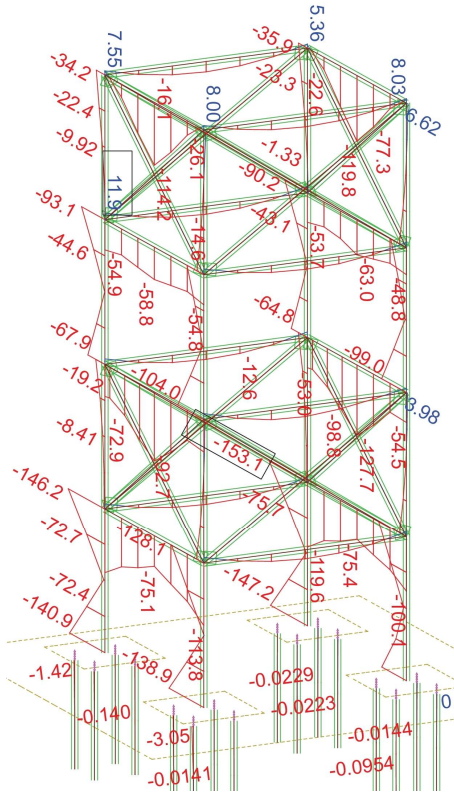


Fig. 13. Envelope diagram (min value) of "elastic" bending moments, $kN \cdot m$

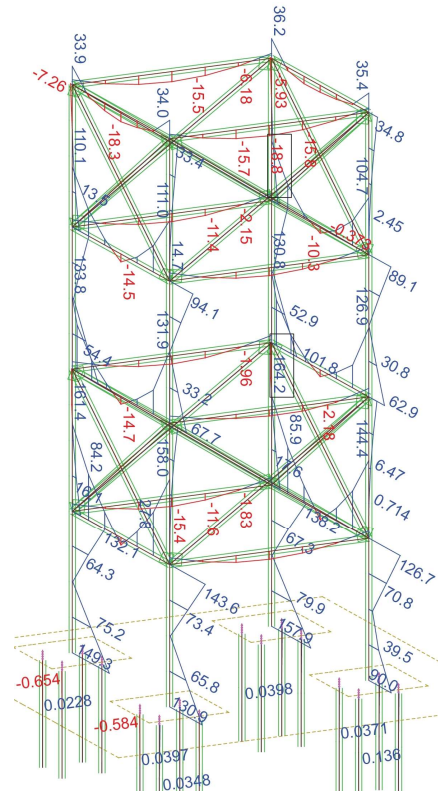


Fig. 14. Envelope diagram (max value) of "elastic" bending moments, $kN \cdot m$

Table 4: Comparison of results

Result	Elastic Analysis	Shakedown Analysis (safety factor 1.19)
Moments in the bottom column M_{max} , $kN \cdot m$	149.3	169
Moments in the bottom column M_{min} , $kN \cdot m$	-140.9	-177.3
Moments in the center of bottom beam M_{min} , $kN \cdot m$	-74.1	-89.7
Moments in the right side of bottom beam M_{min} , $kN \cdot m$	-114	-192.1

Moments in the right side of bottom beam Mmax, kN·m	161.4	146.5
Normal forces in piles Nmin, kN	-105	-110
Moments in the bottom column Mmax, kN·m		

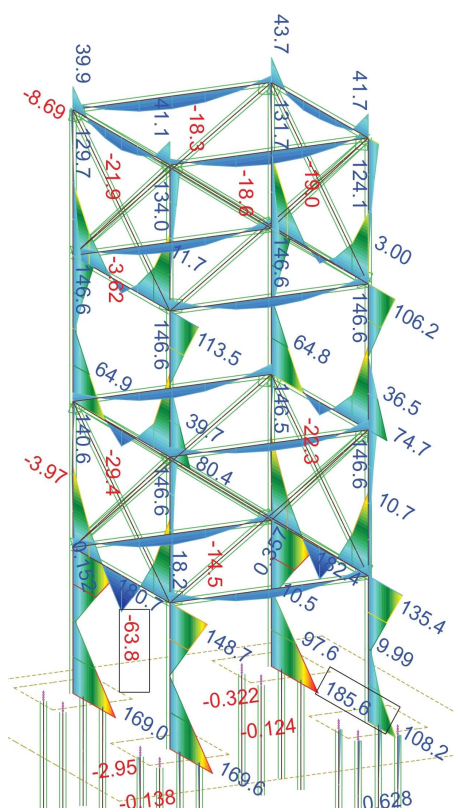


Fig. 15. Envelope moments diagram (max value) after limited plastic redistribution of forces, $kN \cdot m$

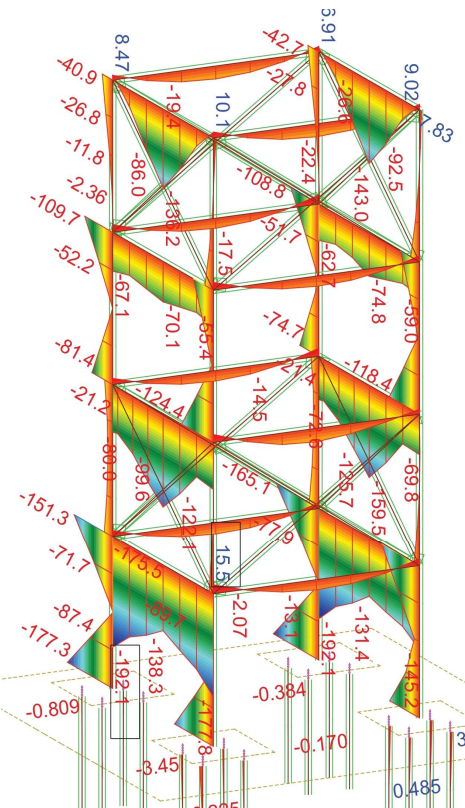


Fig. 16. Envelope moments diagram (min value) after limited plastic redistribution of forces, $kN \cdot m$

4. FLOWCHART OF SEISMIC SHAKEDOWN ANALYSIS

Summarizing the above calculations, we can compose a general sequence of seismic shakedown analysis. General flowchart is shown on Figure 19.

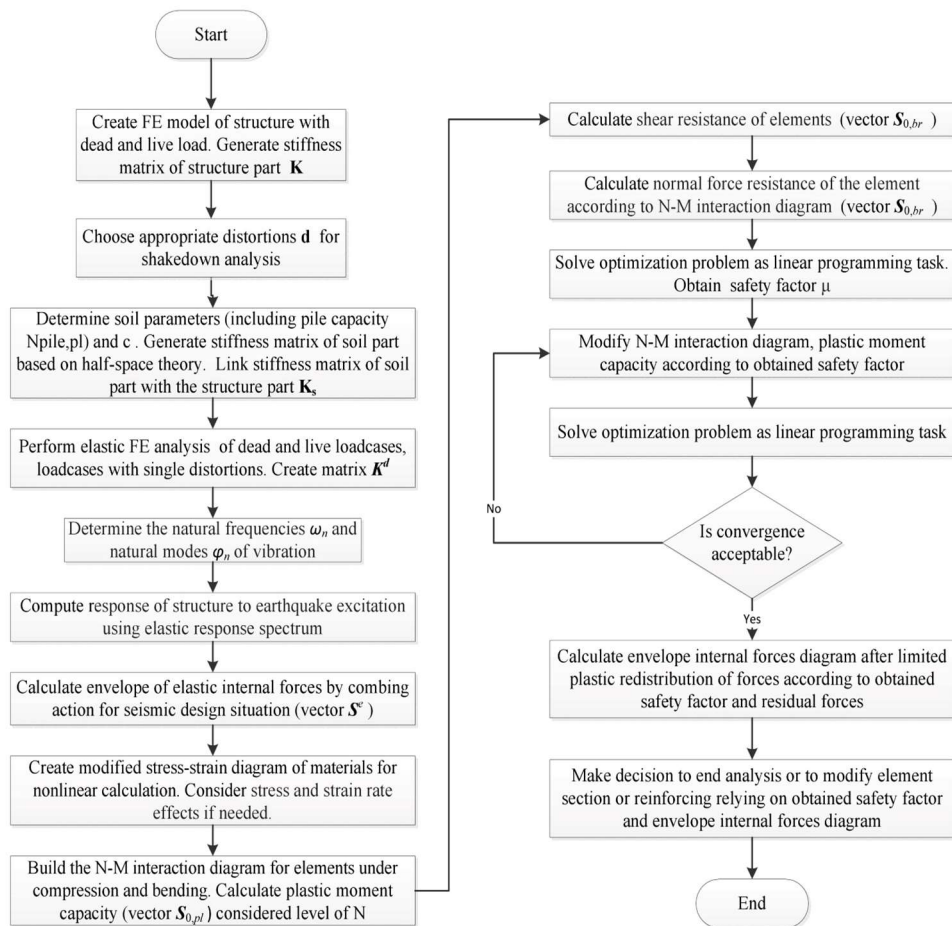


Fig. 17. General flowchart of seismic shakedown analysis

5. CONCLUSIONS

The shakedown FEM analysis of reinforced concrete and composite spatial frame structures on the deformable foundation allows estimating the guaranteed reserves of seismic load bearing capacity of constructions. The elastic-plastic and brittle behavior of structures elements as well as elastic-perfectly plastic behavior of the piles in the soil produce the nonlinear response of systems. The proposed here method will be further generalized to account for the random and uncertain properties of the actions, loads and design parameters of structures.

REFERENCES

1. NIST GCR 12-917-21 (2012) *Soil-Structure Interaction for Building Structures*, Gaithersburg, National Institute of Standards and Technology.
2. Alawdin, Piotr, Bulanov, G. V. (2016) *Shakedown seismic analysis of composite steel concrete frame system // In: Recent Progress in Steel and Composite Structures: Proceedings of the XIII International Conference on Metal Structures, London, Taylor & Francis Group, pp. 231--236.*
3. General Services Administrations (GSA) (2003), *Progressive Collapse Analysis and Design Guidelines for New Federal Office Buildings Major Modernizations Projects.*
4. Bellmann, J. and Radmanovi'c B. (2011) Nonlinear Half-Space Contact. *Proceedings of Structural Engineering World Congress, Italy.*
5. Smolczyk, U. (1980) *Grundbau Taschenbuch.* Wilhelm Ernst & Sohn.
6. Chopra, A.K. and Goel, R.K. *A modal pushover analysis procedure to estimate seismic demands for buildings: theory and preliminary evaluation.* PEER Report 2001/03. [s.l.]. Pacific Earthquake Engineering Research Center. 2001.
7. Eurocode 0: *Basis of structural design*, Brussels, European Committee for standardizations, 2002.
8. *Model Code 2010.* Vol.2. Lausanne: the International Federation for Structural Concrete (fib). 2012.
9. Eurocode 4: *Design of composite steel and concrete structures for. Part 1-1: General rules and rules for buildings*, Brussels, European Committee for standardizations 2005.
10. *Caltrans Seismic Design Criteria*, Version 1.7, Caltrans, 2013.
11. Eurocode 2: *Design of concrete structures. Part 1-1: General rules and rules for buildings*, Brussels, European Committee for standardizations, 2004.
12. Jia, Junbo. (2017) *Modern earthquake engineering: Offshore and land-based structures*, Springer-Verlag, Berlin, Heidelberg.
13. Application of high strength steels in seismic resistant structures: *Proceedings of the Workshop: Naples, Italy, June 28-29, 2013*, Eds. Dan Dubina, Raffaele Landolfo, Aurel Stratan, Cristian Vulcu, "Orizonturi Universitare" Publishing House, Timisoara, Romania, 2014.
14. Elnashai, Amr S., Di Sarno L. (2008) *Fundamentals of earthquake engineering*, Wiley, Ltd, Publication.
15. *Computational methods in earthquake engineering*, Eds. Manolis Papadrakakis, Michalis Fragiadakis, Nikos D. Lagaros, Springer, 2011.
16. *Encyclopedia of earthquake engineering*, Eds. M. Beer, E. Patelli, I. Kougioumtzoglou and I.Siu-Kui Au. Springer, New York, Dordrecht, London, Berlin, 2015.

17. Atkočiūnas, Juozas. (2011) *Optimal shakedown design of elastic-plastic structures*. Vilnius: Technika.
18. Alawdin, P.W. (2005) *Limit analysis of structures under variable loads*. Minsk: UP «Technoprint».
19. *Inelastic analysis of structure under variable loads: Theory and engineering applications*, Eds. D. Weichert, G. Maier, Kluwer Academic Publishers, 2000. (Solid Mechanics and Its Applications, Vol. 83).

PRZYSTOSOWANIE UKŁADU „PODŁOŻE GRUNTOWE-PALE-RAMA” PRZY ODDZIAŁYWANIACH SEJSMICZNYCH

Streszczenie

W niniejszym artykule za pomocą metody elementów skończonych przedstawiona analiza przystosowania sejsmicznego przestrzennych układów ramowych na podłożu odkształcanym, biorąc pod uwagę sprężysto-plastyczne i kruche zachowanie elementów układu. Podłoże składa się z grupy pali w gruncie. Grunt zachowuje się jako sprężyste ciało półprzestrzenne. W modelu odkształcenia pali założono zachowanie idealnie sprężysto-plastyczne, a nośność graniczna pali określa się na podstawie wyników badań podłoża lub samych pali. Przedstawiono przykład przystosowania sejsmicznego dla opisanego wyżej układu ramowego.

Słowa kluczowe: oddziaływania sejsmiczne, przystosowanie, ramy na podłożu odkształcanym, pali, sprężysto-plastyczne i kruche elementy

Editor received the manuscript: 22.03.2018